Theor Chem Acc (2001) 107:27–32
DOI 10.1007/s002140100296

Theoretical
Chemistry Accounts

Regular article

Ab initio calculations for the potential curves and spin–orbit coupling of Mg_2

E. Czuchaj[1], **M. Krośnicki**[1], **H. Stoll**[2]

[1] Institute of Theoretical Physics and Astrophysics, University of Gdańsk, ul. Wita Stwosza 57, 80-952 Gdańsk, Poland
[2] Institut für Theoretische Chemie, Universität Stuttgart, Pfaffenwaldring 55, 70550 Stuttgart, Germany

Received: 10 May 2001 / Accepted: 15 August 2001/Published online: 30 October 2001

Abstract. The ground state and several low-lying excited states of the Mg_2 dimer have been studied by means of a combination of the complete-active-space multiconfiguration self-consistent-field (CASSCF)/CAS multireference second-order perturbation theory (CASPT2) method and coupled-cluster with single and double excitations and perturbative contribution of connected triple excitations [CCSD(T)] scheme. Reasonably good agreement with experiment has been obtained for the CCSD(T) ground-state potential curve but the dissociation energy of the only experimentally known $A^1\Sigma_u^+$ excited state of Mg_2 is somewhat overestimated at the CASSCF/CASPT2 level. The spectroscopic constants D_e, R_e and ω_e deduced from the calculated potential curves for other states are also reported. In addition, some spin–orbit matrix elements between the excited singlet and triplet states of Mg_2 have been evaluated as a function of internuclear separation.

Key words: Collison complexes – Dimers – Potential curves – Spin–orbit coupling

1 Introduction

The alkaline-earth dimers attract special interest owing to the different structures of their weak van der Waals ground state and quite strongly bound excited states. This causes spectral transitions between the excited states and the ground state to appear as broad continua that are shifted far to the red of the corresponding atomic lines. Transitions of this type are very well suited for laser applications. Ab initio potential curves and spin–orbit (SO) coupling matrix elements are crucial for interpretation of various experiments performed on these systems and for more realistic theory. Recently, interest in the alkaline-earth dimers has grown because of the possibility of using these diatomics in studies of collisions of cold atoms. Cold collisions of the aforementioned atoms offer, among others, the prospects of quantitative experiments and theory on small-detuning trap loss, high-resolution photoassociation spectroscopy on several molecular states and optical shielding experiments. In particular, the *R*-dependent SO matrix elements provide the basic magnitude of the fine-structure changing mechanism for trap loss rates observed in magnetooptical traps and the widths of photoassociative spectroscopy [1]. In general, the molecular structure involving low-lying states of the alkaline-earth dimers is fairly well known from spectroscopic studies. So far, a few ab initio calculations on the potential curves of species such as Mg_2, Sr_2 and Ba_2 have appeared in the literature. On the other hand, the SO coupling for these species as a function of internuclear separation has not been investigated. The present study is devoted to the Mg_2 dimer. We chose this system because the number of electrons in this case is sufficiently low to allow reasonably accurate ab initio calculations. The Mg_2 dimer was investigated earlier, both experimentally and theoretically. In particular, the absorption spectrum of this molecule was measured by Balfour and Douglas [2]. These authors found an extensive rovibrational spectrum in the 3500-Å region which was assigned to an $A^1\Sigma_u^+ \leftarrow X^1\Sigma_g^+$ transition. In addition, the absorption band was found to extend to wavelengths considerably shorter than the Mg resonance line at 2852 Å but this region appeared more complex and was not fully understood. Based on a Rydberg–Klein–Rees (RKR) procedure, experimental values for the spectroscopic constants of the $X^1\Sigma_g^+$ ground state and the $A^1\Sigma_u^+$ excited state of Mg_2 were deduced from the measured spectrum. The measurements of Balfour and Douglas were subsequently reevaluated by Vidal and Scheingraber [3] by means of an improved variational procedure. On the theoretical side, ab initio calculations on Mg_2 were performed by several authors. Stevens and Krauss [4] carried out multiconfiguration self-consistent-field (MCSCF) calculations for the ground state and lower-

Correspondence to: E. Czuchaj

lying excited triplet and singlet states. The resulting theoretical dissociation energies for the $X^1\Sigma_g^+$ and $A^1\Sigma_u^+$ states of Mg_2 proved, however, to be in poor agreement with experiment, which indicated the importance of correlation effects in molecular calculations. Another ab initio calculation for the potential curves of Mg_2 comprising both the ground state and excited states was performed by Jones [5], who used for this purpose the local spin-density functional method. Like in the previous case, his results deviate appreciably from available experimental data. As a rule, the density functional approach provides overestimated values for the binding energy. Other calculations on Mg_2 [6–9] were restricted only to the ground state and yielded distinctly overestimated dissociation energies. To the best of our knowledge, no other calculations have appeared on the excited states of Mg_2; therefore, calculation of the potential curves for Mg_2 at a higher level of theory is still of interest.

The main goal of the present study is to calculate the potential energies for the low-lying excited triplet and singlet states of Mg_2. We hope that our results will be helpful in future experimental and theoretical investigations. We calculated potential curves for the Mg_2 states arising from the $(3s^2)^1S + {}^1S$, $(3p)^3P + {}^1S$ and $(3p)^1P + {}^1S$ atomic asymptotes as well as for a higher $^1\Pi_u$ state correlating to the $(3p)^3P + {}^3P$ asymptote. The calculations were carried out at the complete-active-space MCSCF (CASSCF)/CAS multireference (MR) second-order perturbation theory (CASPT2) level with 24 correlated electrons, using a large basis set containing up to g functions. In addition, the SO matrix elements between the excited singlet and triplet states of Mg_2 versus internuclear separation were evaluated at the MR configuration interaction (CI) level. After a brief presentation of the calculational details in Sect. 2, the results obtained are discussed in the context of available experimental data in Sect. 3.

2 Computational details

The CASSCF/CASPT2 calculations for Mg_2 reported here were carried out with the MOLPRO program of Werner and Knowles [10–14]. In the CASSCF method the spatial parts of the molecular orbitals are expanded in a basis of Gaussian-type functions. We used the standard correlation-consistent polarized valence quintuple-zeta basis set for Mg augmented by additional diffuse functions with exponents 0.013006, 0.005731 for *s* symmetry, 0.009586, 0.004622 for *p* symmetry and 0.05, 0.022727 for *d* symmetry. The diffuse exponents were determined by means of even-tempered continuation of the series of low exponents in each case. The final contracted basis set for Mg is designated as (22s16p6d3f2g)/[16s14p6d3f2g]. The quality of the basis set was examined in CI calculations for the ground state and several excited states of the Mg atom. For that purpose, the SO-averaged atomic energies were calculated in the *LS* coupling scheme by means of the CASSCF method followed by the CASPT2 method. The 12 electrons of the Mg atom were distributed among the $1s2s2p$ core and the $3s3p$ valence orbitals to form an appropriate active space in the D_{2h} point group. In the CASSCF calculations, the $1s2s2p$ orbitals were kept doubly occupied in all configuration state functions (CSFs). They were, however, fully optimized in MCSCF calculations and correlated in the subsequent CASPT2 calculations through single and double excitations from the reference CSFs. The calculated excitation energies for Mg from the $(3s^2)^1S$ ground state to the excited $(4s)^1S$, $(4s)^3S$, $(3p)^1P$ and $(3p)^3P$ states are 43133 (43503), 41636 (41197), 34857 (35051) and 21721 (21891) cm^{-1}, respectively. The numbers in parentheses denote the experimental values [15].

The potential curves for Mg_2 were calculated in the ΛS coupling scheme using the CASSCF method to generate the orbitals for the subsequent CASPT2 calculations with an open-shell correction term to the one-electron Fock operator as proposed by Werner [14]. In the present calculations, we used a more efficient second-order program written by Celani and Werner [16] in which also subspaces of the singly external and internal configuration spaces are internally contracted. The corresponding active space in the C_{2v} point group consisted of the molecular counterparts of the $1s2s2p$ core, $3s3p$ valence and $4s4p$ Rydberg orbitals of the Mg atom among which 24 electrons were distributed. The inclusion of the $4s4p$ orbitals in the active space was necessary to improve convergence of the CASPT2 calculations, especially in an intermediate range of internuclear separation. Ultimately, the CASSCF reference wavefunctions were built from four valence electrons distributed among 16 molecular orbitals ($4\sigma_g$, $4\sigma_u$, $5\sigma_g$, $5\sigma_u$, $2\pi_u$, $2\pi_g$, $6\sigma_g$, $6\sigma_u$, $7\sigma_g$, $7\sigma_u$, $3\pi_u$, $3\pi_g$). The molecular orbitals were determined in a state-averaged CASSCF with the same weight for the ground and excited states. The basis set superposition error, although of minor importance for the excited states, was eliminated by means of the standard counterpoise method of Boys and Bernardi [17]. In addition, some SO matrix elements between the excited singlet and triplet states of Mg_2 were computed at the MRCI level using the Breit–Pauli (BP) operator. In the calculations, the full BP operator is used only for computing the matrix elements between internal configurations (no electrons in external orbitals), while for contributions of external configurations a mean-field one-electron Fock operator is employed [13]. In the SO calculations the basis g-type functions were omitted.

3 Results and discussion

The molecular calculations were performed for the Mg_2 dimer in the internuclear separation range from 3.25 to $40a_0$ with different step sizes. The calculations involve the ground state and nine low-lying excited states. The potential energies were calculated with respect to the corresponding energies of the separated atoms at $R = 100a_0$. The potential curves are plotted in Figs. 1, 2 and 3. In Fig. 2 the asymptotic energy for each state was set equal to the experimental energy of the separated atoms. Numerical values of the potential energies are available from the authors (E.C.) upon request. In turn, the potential depths, D_e, and equilibrium positions, R_e, were determined using a cubic spline approximation to the calculated potentials around their equilibrium positions. Moreover, to obtain the fundamental frequencies, ω_e, we employed the calculated potentials in the radial Schrödinger equation for nuclear motion, which was then solved numerically with the Numerov–Cooley method. The spectroscopic constants derived from the calculated potential energies for Mg_2 are listed in Table 1. On the whole, we obtained qualitative agreement between our potential curves and those of Steven and Krauss [4], although some quantitative differences occur.

3.1 Ground state

The $X^1\Sigma_g^+$ ground state of Mg_2 arises from two $(3s^2)^1S$ Mg atoms and, in general, is represented by the single configuration wavefunction [core] $4\sigma_g^2 4\sigma_u^2$, where [core] represents the electronic configuration of the inner shell

electrons. For the ground state, the only possible long-range attractive force between the two atoms is due to the dispersion interaction caused by correlations between the fluctuating multipolar charge distributions of the atoms. In the region of intermediate internuclear separations where the molecule is formed, covalent bonding also contributes to the interaction energy. In the present study, the CASPT2 dissociation energy of the ground state proved to be underestimated about 20%. In order to obtain a better result, we recalculated the ground-state potential energy for Mg_2 using the coupled-cluster with single and double excitations and perturbative contribution of connected triple excitations [CCSD(T)] scheme for all 24 correlated electrons. The resulting CCSD(T) ground-state dissociation energy, $D_e = 404\,cm^{-1}$, for Mg_2 agrees reasonably well with the RKR experimental value of $D_e = 424 \pm 5\,cm^{-1}$ [2] but the calculated bond length, $R_e = 7.50a_0$, somewhat exceeds the experimental value of $R_e = 7.35a_0$. Other theoretical results for D_e of the Mg_2 ground state ($620\,cm^{-1}$ [4], $887\,cm^{-1}$ [5], $459\,cm^{-1}$ [7], $475\,cm^{-1}$ [9]) clearly exceed the experimental value. The calculated CCSD(T) ground-state potential curve for Mg_2 is plotted in Fig. 1.

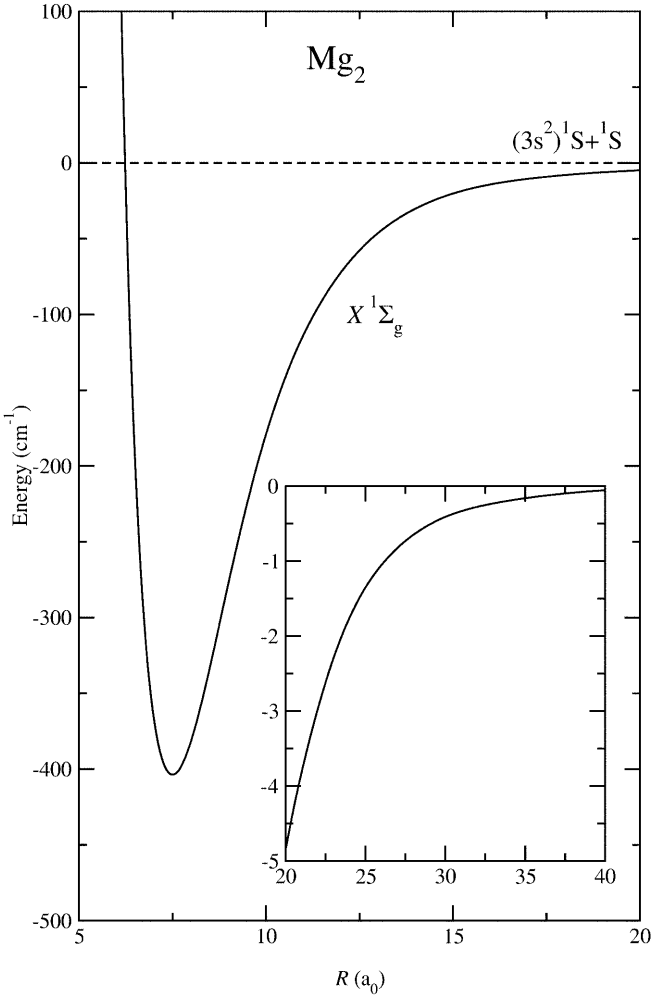

Fig. 1. Ground-state potential curve for the Mg_2 dimer

Table 1. Spectroscopic constants D_e (cm^{-1}), R_e (Bohr) and ω_e (cm^{-1}) of the Mg_2 potential curves arising from the $^1S + {}^1S$, $^1P + {}^1S$ and $^3P + {}^1S$ asymptotes

State	D_e	R_e	ω_e
$X^1\Sigma_g^+$	404 (424 ± 5)[a]	7.50 (7.35)[a]	45.4 (51.12)[a]
$^1\Sigma_u^+$	10480 (9387)[a]	5.85 (5.82)[a]	191.5 (190.6)[a]
$^1\Pi_u$	8460	5.35	252.0
$(2)^1\Sigma_g^+$	6110	6.00	162.4
$^1\Pi_g$	18600	5.15	286.9
$^3\Sigma_g^+$	67	11.75	15.3
$^3\Pi_u$	260	8.00	34.4
$^3\Sigma_u^+$	8090	5.65	228.1
$^3\Pi_g$	8572	5.25	259.3

[a] Ref. [2]

3.2 Singlet states

The singlet excited states of Mg_2 considered in this study are primarily those which arise from the valence $^1P + {}^1S$ atomic asymptote. The calculations show, however, that Rydberg-valence mixing is significant for the excited states which contributes appreciably to the binding energy of these states. The long-range part of the interaction of two like atoms in different energy states is dominated by the electrostatic dipole–dipole resonance energy. The leading term of the first-order dipole–dipole resonance energy is proportional to the $d_z^2R^{-3}$ term, where d_z^2 is the square of the dipole transition moment between the ground state and the excited state of the atom [18]. The only experimentally known excited state of Mg_2 is $A^1\Sigma_u^+$. This state strongly couples with the ground state as a result of electric dipole transitions. Asymptotically, the $A^1\Sigma_u^+$ state is described by the $4\sigma_g^2 4\sigma_u 5\sigma_g$ and $4\sigma_g 4\sigma_u^2 5\sigma_u$ configurations and the long-range part of its interaction energy is dominated by the $-2d_z^2R^{-3}$ term. Comparing the potential energy of the $A^1\Sigma_u^+$ state calculated at $R = 40a_0$ to its leading asymptotical term yields the corresponding $d_z^2 = 4.67$ au, which agrees roughly with the experimental value of 5.67 au, as quoted by Stevens and Krauss [4], and our CASSCF/CI value of 5.61 au. The calculated bond strength of the $A^1\Sigma_u^+$ potential curve is $10480\,cm^{-1}$ and exceeds the RKR experimental value [2, 3] by about $1080\,cm^{-1}$. Quite good agreement occurs, however, for the bond length (Table 1). Another excited state of Mg_2 which strongly couples with the ground state is $^1\Pi_u$. The asymptotic configurations describing this state are $4\sigma_g 4\sigma_u^2 2\pi_u$ and $4\sigma_g^2 4\sigma_u 2\pi_g$. The long-range part of the interaction energy of the $^1\Pi_u$ state is dominated by $d_z^2R^{-3}$. The CASPT2 calculation for some points of the $^1\Pi_u$ potential curve, particularly in the region $8–10a_0$, appeared to be strongly divergent. This divergence problem was easily removed by including the $4s4p$ orbitals into the active space and by simultaneous calculation of two states of $^1\Pi_u$ symmetry. The higher of them correlates to the $^3P + {}^3P$ limit described asymptotically by the $4\sigma_g^2 5\sigma_g 2\pi_u$ and $4\sigma_u^2 5\sigma_g 2\pi_u$ configurations in which two electrons occupy a p-type molecular orbital. As seen in Fig. 2, the two states

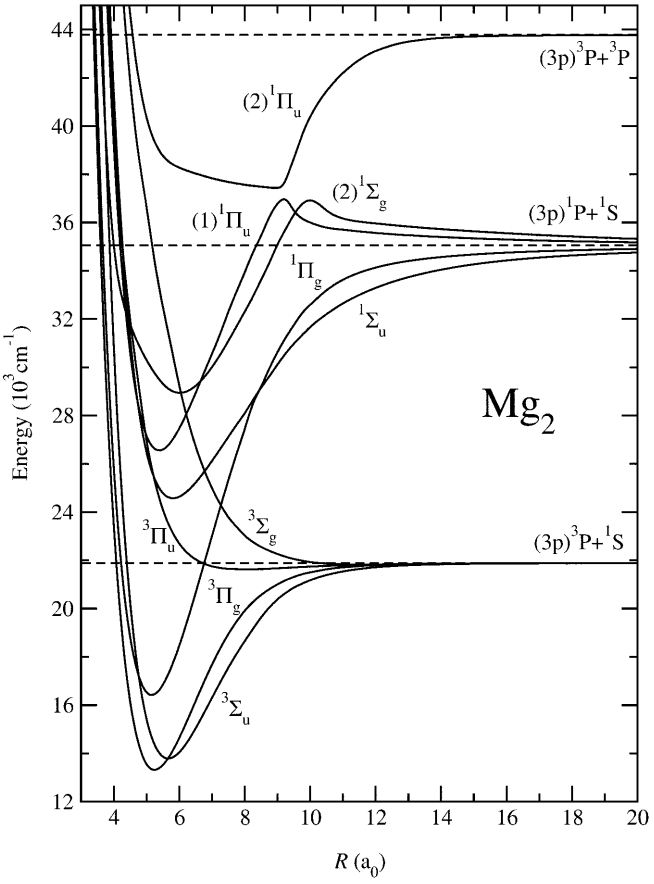

Fig. 2. Potential curves for the excited triplet and singlet states of the Mg_2 dimer arising from the $^3P + {}^1S$ and $^1P + {}^1S$ asymptotes

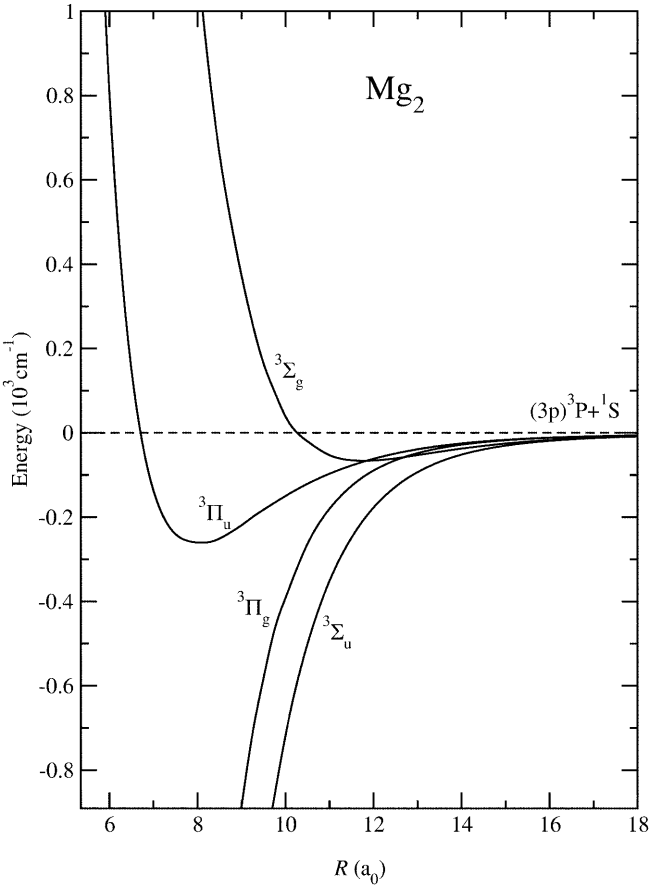

Fig. 3. Triplet potential curves of Mg_2 in an intermediate range of internuclear separation

exhibit an avoided crossing at $R = 9a_0$. Owing to that, the lower $^1\Pi_u$ state becomes strongly bound, with a minimum located at $R_e = 5.35a_0$. Besides, near the avoided crossing the lower $^1\Pi_u$ potential curve exhibits a barrier of about $1900\,cm^{-1}$ above the dissociation energy. The shape of the $^1\Pi_u$ potential curves allows the absorption spectrum of Mg_2 measured by Balfour and Douglas and identified as the $A^1\Sigma_u^+ \leftarrow X^1\Sigma_g^+$ band [2] to be understood. This rovibrational spectrum centered primarily in the 3500 Å region extends to wavelengths shorter than the resonance line of Mg (2852 Å). Aside from weak rovibrational bands, this spectrum becomes diffuse with decreasing wavelengths but has a well-defined absorption edge at 2660 Å which now can be assigned to transitions to the quasibound levels of the lower $^1\Pi_u$ state. In view of the present results, it seems evident that the experimental 3500-Å absorption spectrum of Mg_2 which was reported as consisting of many overlapping bands, extending considerably above the resonance line of Mg and displaying a complex structure, particularly in the region of short wavelengths, should be assigned not only to dipole transitions from the ground state to the $A^1\Sigma_u^+$ state but also to both the $^1\Pi_u$ states.

The $(2)^1\Sigma_g^+$ state of Mg_2 is asymptotically described by the $4\sigma_g 4\sigma_u^2 5\sigma_g$ and $4\sigma_g^2 4\sigma_u 5\sigma_u$ configurations. A simple molecular orbital analysis shows that such a state is expected to be not strongly bound. Contrary to that our calculations show that this state possesses a substantial amount of binding energy arising from admixture of higher-lying configurations. In addition, the $(2)^1\Sigma_g^+$ potential curve exhibits a sizeable barrier at $R = 10a_0$ as a result of the long-range dipole–dipole resonance forces proportional to $2d_z^2R^{-3}$. Finally, the most attractive singlet state of Mg_2 is $^1\Pi_g$, which asymptotically is described by the $4\sigma_g^2 4\sigma_u 2\pi_u$ and $4\sigma_g 4\sigma_u^2 2\pi_g$ configurations. The long-range dipole–dipole resonance attraction of this state is represented by the $-d_z^2R^{-3}$ term. For shorter internuclear distances, the calculations yield a very strong bond strength for the $^1\Pi_g$ state as a result of valence bonding and admixture of Rydberg states. The spectroscopic constants of the valence states of Mg_2 are listed in Table 1.

3.3 Triplet states

The most attractive triplet state of Mg_2 is $^3\Pi_g$, which is asymptotically described by the same two configurations as the $^1\Pi_g$ state except for spin coupling. This state is metastable with respect to electric dipole transitions to the ground state and can serve as a molecular reservoir when used in laser applications. Another strongly bound triplet state of Mg_2 is $^3\Sigma_u^+$, described asymptotically by the same configurations as the $^1\Sigma_u^+$ state. This state is the lowest-lying excimer state which can radiate to the

ground state owing to SO mixing with the $^1\Pi_u$ state. In turn, the $^3\Pi_u$ state is represented asymptotically by the two configurations which describe the $^1\Pi_u$ state. This state is unbound with only a shallow minimum of $260\,\mathrm{cm}^{-1}$ at $R_e = 8a_0$. Finally, the $^3\Sigma_g^+$ state represented asymptotically by the same configurations as the $(2)^1\Sigma_g^+$ state is the most repulsive state of all Mg_2 triplet states. At larger internuclear distances the $^3\Sigma_g^+$ potential curve is almost flat with only a shallow minimum of $67\,\mathrm{cm}^{-1}$ at $R_e = 11.75a_0$. The triplet potential curves in an intermediate range of internuclear separation are shown in Fig. 3. In the present study we did not consider the SO structure of the interaction energy. The potential curves reported are sufficient for some further applications, for example, for obtaining cross-sections for non-adiabatic transitions between the singlet and triplet states of Mg_2 by means of quantum scattering methods based on close-coupling calculations [1]. If necessary, the present potential curves could be easily split into fine-structure components by applying a simple semiempirical technique called "atoms in molecules" [19]. The basic assumption of this technique is, however, that SO coupling is independent of R.

The SO matrix elements calculated in this work are prompted by the recent studies, both experimental and theoretical, of light-induced collisions between cold, neutral alkaline-earth atoms in magneto-optical traps [1]. SO coupling which mixes the singlet and triplet states of an alkaline-earth dimer plays an important part in cold collisions. Since its dependence on internuclear separation is unknown, it is commonly assumed to be independent of R. Such an assumption is, of course, too simplified. Therefore, evaluation of the SO coupling for Mg_2 versus R is of interest. The most important SO matrix elements of Mg_2 calculated as a function of R between the excited singlet and triplet states are plotted in Fig. 4. Their numerical values are available upon request. As seen from the figure, the SO coupling for Mg_2 exhibits rather strong dependence on R, particularly in the range of shorter internuclear separation. Asymptotically, all three matrix elements tend gradually to the sscorresponding atomic values. Two of them, $\langle {}^1\Sigma_u|\mathrm{SO}|{}^3\Pi_u\rangle$ and $\langle {}^1\Pi_g|\mathrm{SO}|{}^3\Sigma_g^+\rangle$ decrease rapidly with decreasing R to pass zero in the region $4.5 - 5.0a_0$. In turn, the $\langle {}^1\Pi_g|\mathrm{SO}|{}^3\Pi_g\rangle$ matrix element exhibits a shallow minimum at about $R = 8a_0$ and rises strongly with decreasing R. For comparison, the present calculations yield the $(3p)^3\mathrm{P}_1 - (3p)^3\mathrm{P}_0$ energy splitting for the Mg atom to be $15.37\,\mathrm{cm}^{-1}$ as compared with its experimental value of $20.06\,\mathrm{cm}^{-1}$ [15].

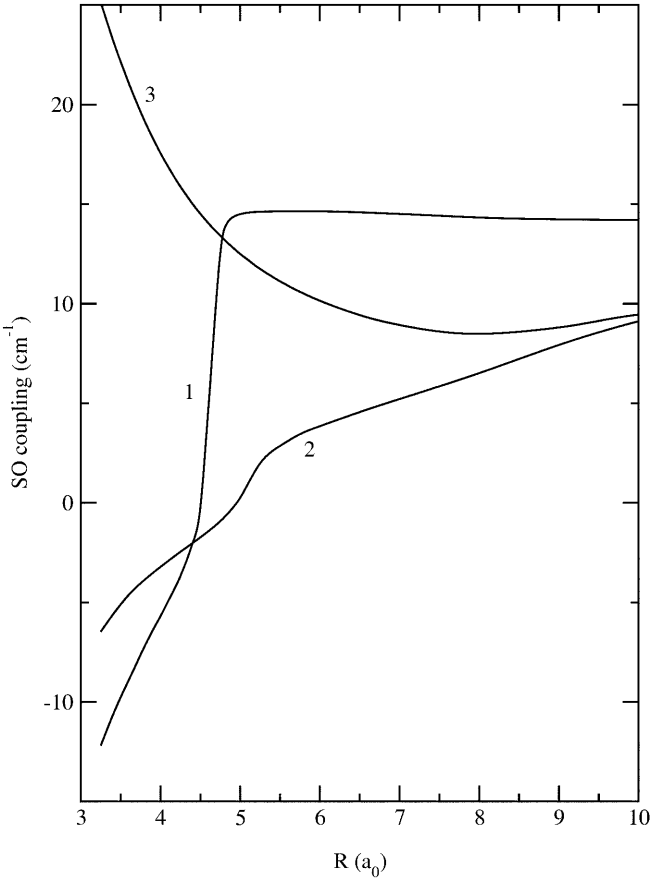

Fig. 4. Spin–orbit (SO) matrix elements calculated as a function of internuclear separation: $\langle {}^1\Sigma_u^+|\mathrm{SO}|{}^3\Pi_u\rangle$ (*1*), $\langle {}^1\Pi_g|\mathrm{SO}|{}^3\Sigma_g^+\rangle$(*2*), $\langle {}^1\Pi_g|\mathrm{SO}|{}^3\Pi_g\rangle$(*3*)

In order to verify the quality of the present CASPT2 calculations for Mg_2 we checked what one obtains at the CASPT3 level of correlation treatment [14]. Unfortunately, the present version of the MOLPRO code is unable to perform CASPT3 calculations in an active space consisting of more than 16 active orbitals; hence our CASPT3 calculations had to be performed in an active space reduced to the valence orbitals. On the whole, the calculated PT3 potential curves nearly agree with their PT2 counterparts asymptotically and in a range of very short internuclear distances. Some substanial differences occur between the two sets of potential curves in an intermediate range of internuclear separation. First of all, the PT3 singlet potential curves are moved up with respect to the corresponding PT2 potential curves by more than $1000\,\mathrm{cm}^{-1}$. In turn, the PT3 triplet potential curves are moved down by roughly the same amount of energy. Besides, whereas the PT3 singlet and triplet potential curves of Σ_u^+ and Π_g symmetries behave regularly versus R over the entire range of internuclear separation, the Σ_g^+ and Π_u ones display strong irregularity over an intermediate range of R. However, the bond strength of the PT3 potential curve of the $A^1\Sigma_u^+$ state ($D_e = 9420\,\mathrm{cm}^{-1}$) turns out to be in reasonable agreement with the experimental value (Table 1). On the other hand, the PT3 potential curves for the $^3\Sigma_g^+$ and $^3\Pi_u$ states possess surprisingly deep minima lying about $1500\,\mathrm{cm}^{-1}$ below the dissociation limit and cannot be accepted as trustworthy. In our opinion, a larger active space in the CASPT3 calculations should remove the current numerical difficulties. It is also interesting to quote our PT2 and PT3 results for Mg_2 obtained within the four-electron model plus the energy-consistent pseudopotential supplemented by the core polarization potential. The resulting potential curves are surprisingly consistent with our former PT2

results for all the Mg_2 states considered. Moreover, unlike in the 24-electron model, there is now a very small difference between the PT2 and PT3 potential curves. For example, the bond strength of the $^1\Sigma_u^+$ state calculated within the four-electron model amounts to $10750\,cm^{-1}$, which differs only slightly from the PT3 result ($10680\,cm^{-1}$) and is reasonably consistent with our former PT2 value of $10480\,cm^{-1}$. For the remaining states of Mg_2 the situation is similar. In light of the previous discussion our PT2 potential curves for Mg_2 obtained with the 24-electron model seem to be the most reliable at the present stage of the calculations, although correlation treatment at the CASPT2 level is certainly insufficient.

4 Conclusions

The low-lying valence states of the Mg_2 dimer were studied by a combination of the CASSCF/CASPT2 and CCSD(T) methods. The calculated CCSD(T) ground-state potential curve is reasonably consistent with the corresponding experimental RKR curve. Somewhat poorer agreement was obtained at the CASSCF/CASPT2 level for the $A^1\Sigma_u^+$ state of Mg_2. All states arising from the $^1P + {}^1S$ asymptote are strongly bound, which leads to crossing with the lower-lying triplet states. In addition, the SO matrix elements between excited singlet and triplet were computed versus R at the MRCI level using the BP operator. To the best of our knowledge, the present results on the SO coupling for Mg_2 are the first such results for the alkaline-earth dimers. They are believed to be of importance for future studies of the Mg_2 dimer, especially with respect to trap loss effects taking place in a magnetooptical trap.

Acknowledgements. This work was supported by the KBN under grant no. 5 P03B 082 21 E.C. thanks W. Miklaszewski for his help with the numerical calculations.

References

1. Machholm M, Julienne PS, Suominen K-A (1999) Phys Rev A 59: R4113
2. Balfour WJ, Douglas AE (1970) Can J Phys 48: 901
3. Vidal CR, Scheingraber H (1977) J Mol Spectrosc 65: 46
4. Stevens WJ, Krauss M (1977) J Chem Phys 67: 1977
5. Jones RO (1979) J Chem Phys 71: 1300
6. Chałasiński G, Funk DJ, Simons J, Breckenridge WH (1987) J Chem Phys 87: 3569
7. Dyall KG, McLean AD (1992) J Chem Phys 97: 8424
8. Klopper W, Almlöf J (1993) J Chem Phys 99: 5167
9. Tao F-M, Pan Y-K (1994) Mol Phys 81: 507
10. Werner H-J Knowles PJ, with contributions from Amos RD, Berning A, Cooper DL, Deegan MJO, Dobbyn AJ, Eckert F, Hampel C, Hetzer G, Leininger T, Lindh R, Lloyd AW, Meyer W, Mura ME, Nicklass A, Palmieri P, Peterson K, Pitzer R, Pulay P, Rauhut G, Schütz M, Stoll H, Stone AJ, Thorsteinsson T MOLPRO (a package of ab initio programs) University of Birmingham, UK
11. Werner H-J, Knowles PJ (1985) J Chem Phys 82: 5053
12. Knowles PJ, Werner H-J (1985) Chem Phys Lett 115: 259
13. Berning A, Werner H-J, Palmieri P, Knowles PJ (2000) Mol Phys 98: 1823
14. Werner H-J (1996) Mol Phys 89: 645
15. Moore CE (1958) Atomic energy levels. NSRDS-NBS circular no. 467. US Government Printing Office, Washington, DC
16. Celani P, Werner H-J (2000) J Chem Phys 112: 5546
17. Boys SF, Bernardi F (1970) Mol Phys 19: 553
18. Hirschfelder JO, Meath WJ (1967) In: Hirschfelder JO (ed) Advances in chemical physics, vol 12. Wiley-Interscience, New York, pp 3–106
19. Cohen JS, Schneider B (1974) J Chem Phys 61: 3230